Author Manuscript

Author Manuscript

Author Manuscript

Author Manuscript

HHS Public Access

Author manuscript

Appl Mater Today. Author manuscript; available in PMC 2019 March 01.

Published in final edited form as:

Appl Mater Today. 2018 March ; 10: 194–202. doi:10.1016/j.apmt.2017.12.004.

Functionalization of PCL-3D Electrospun Nanofibrous Scaffolds for Improved BMP2-Induced Bone Formation

Jacob M. Miszuk[a,†], **Tao Xu**[b,†], **Qingqing Yao**[a], **Fang Fang**[c], **Josh D. Childs**[a], **Zhongkui Hong**[a], **Jianning Tao**[c], **Hao Fong**[b,**], and **Hongli Sun**[a,*]

[a]Department of Biomedical Engineering, University of South Dakota, BioSNTR, Sioux Falls, SD 57107, USA

[b]Program of Biomedical Engineering, South Dakota School of Mines and Technology, Rapid City, SD 57701, USA

[c]Children's Health Research Center at Sanford Research, Sioux Falls, SD 57104, USA

Abstract

Bone morphogenic protein 2 (BMP2) is a key growth factor for bone regeneration, possessing FDA approval for orthopedic applications. BMP2 is often required in supratherapeutic doses clinically, yielding adverse side effects and substantial treatment costs. Considering the crucial role of materials for BMPs delivery and cell osteogenic differentiation, we devote to engineering an innovative bone-matrix mimicking niche to improve low dose of BMP2-induced bone formation. Our previous work describes a novel technique, named thermally induced nanofiber self-agglomeration (TISA), for generating 3D electrospun nanofibrous (NF) polycaprolactone (PCL) scaffolds. TISA process could readily blend PCL with PLA, leading to increased osteogenic capabilities *in vitro*, however, these bio-inert synthetic polymers produced limited BMP2-induced bone formation *in vivo.* We therefore hypothesize that functionalization of NF 3D PCL scaffolds with bone-like hydroxyapatite (HA) and BMP2 signaling activator phenamil will provide a favorable osteogenic niche for bone formation at low doses of BMP2. Compared to PCL-3D scaffolds, PCL/HA-3D scaffolds demonstrated synergistically enhanced osteogenic differentiation capabilities of C2C12 cells with phenamil. Importantly, *in vivo* studies showed this synergism was able to generate significantly increased new bone in an ectopic mouse model, suggesting PCL/HA-3D scaffolds act as a favorable synthetic extracellular matrix for bone regeneration.

TOC Image

*Corresponding Authors: Professor Hongli Sun, Ph.D. Phone: (+1) 605-275-7470; Fax: (+1) 605-782-3280; Hongli.Sun@usd.edu.
**Professor Hao Fong, Ph.D. Phone: (+1) 605-394-1229; Fax: (+1) 605-394-1232; Hao.Fong@sdsmt.edu.
†These authors contributed equally to this work.

Publisher's Disclaimer: This is a PDF file of an unedited manuscript that has been accepted for publication. As a service to our customers we are providing this early version of the manuscript. The manuscript will undergo copyediting, typesetting, and review of the resulting proof before it is published in its final citable form. Please note that during the production process errors may be discovered which could affect the content, and all legal disclaimers that apply to the journal pertain.

Author Manuscript Author Manuscript Author Manuscript Author Manuscript

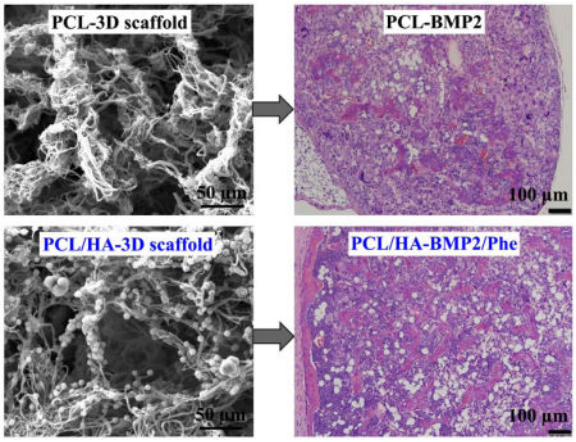

Keywords

3D electrospun nanofibrous scaffold; Hydroxyapatite functionalization; Phenamil; Osteogenic differentiation; Bone Regeneration

1. Introduction

Biomaterials-mediated bone morphogenic proteins (BMPs) delivery for bone graft substitutes is a fast-growing strategy for repair of critical sized bone defects [1–3]. Two FDA approved growth factors, BMP2 and BMP7, are used in orthopedic applications in clinical settings due to their potent ability to induce osteogenesis and bone formation [2]. However encouraging the use of BMPs are in bone regeneration, several factors limit the clinical effectiveness of BMPs in practice; including high dosage requirement, high associated costs, unintended side effects, and other more serious consequences including ectopic bone formation and increased cancer risk [4, 5]. Therefore, it is urgent to develop novel strategies to address these challenges for BMPs application in bone repair.

With an increased understanding of the role of extracellular matrix (ECM) during tissue repair, researchers are recognizing that the fibrous networks are not only providing mechanical support and adhesion sites to cells, but also acting as a reservoir for many growth factors which control a variety of cellular processes [6]. Engineering a 3D scaffold to mimicking the natural ECM for bone regeneration is a critical step in making an effective niche for stem cells and growth factors, as both chemical and physical features of the materials can significantly affect its interaction with cells and BMPs [7]. For example, functional groups and charged surfaces have been shown to impact the adsorption-desorption rate of BMP2 in *in vitro* experiments [8]. The structure of the scaffold can also directly affect growth factors release kinetics, as factors such as fiber diameter, overall porosity, and pore size can significantly impact BMP2-induced bone and cartilage formation [9]. Thus, it is of critical importance to develop innovative and favorable 3D scaffolds for bone tissue engineering [7].

Mimicking the natural ECM of bone has long been a strategy to approach the development of synthetic scaffolds for bone repair; specifically targeting the size and shape of collagen

Author Manuscript Author Manuscript Author Manuscript Author Manuscript

fibers ranging from tens to hundreds of nanometers in diameter, which are the main component of natural bone matrix [10]. Techniques attempting to mimic the structure of natural ECM have arisen over recent years, with methods including self-assembly, phase separation, and more recently notable, electrospinning [11]. Electrospinning technique has gained interest lately due to its ability to generate nanofibers with morphological structures very closely similar to natural ECM as well as robust processing capabilities [12–14]. Electrospun scaffolds possess high surface area and porous structure, two factors helping encourage cell adhesion, migration, and differentiation, making it a viable strategy for tissue engineering scaffolds. However beneficial these characteristics may be, electrospun NF mats lack interconnected macroporous structures critical for the infiltration and growth of cells [15].

Our recently published work describes a novel technique of thermally induced nanofiber self-agglomeration (TISA) followed by freeze drying; a process by which as-electrospun polycaprolactone (PCL) NF mats can be transformed into 3D electrospun PCL NF scaffolds with interconnected macroporous structures [15]. Ensuing *in vitro* and *in vivo* data indicated scaffolds ability to successfully support BMP2-induced osteogenic differentiation and bone formation, however, only limited new bone was identified in the surrounding area of scaffolds [15]. Consequently, our other recent work explored improving the bioactivity of PCL scaffolds by introducing polylactic acid (PLA) blend, showing improved mechanical properties and bioactivity [16]. Although the PCL/PLA-3D scaffolds significantly promoted more osteogenic differentiation *in vitro* and new bone formation *in vivo* than PCL-3D scaffolds, the bone forming ability of the blend scaffolds were still limited and not able to completely heal the critical-sized bone defect even after addition of rhBMP2 [16]. These finding suggested that the bioinert nature of these synthetic polymers (*i.e.*, PCL and PLA) urged more biomimicking-functionalizations to create more bone-forming favorable microenvironment for improving the signaling activity of BMP2 and bone regeneration.

Improvements to PCL scaffolds seek to enhance the BMP2-induced bone formation capabilities of our designs, where we look to functionalize the scaffold and directly activate the BMP2 signaling pathway as well. Bone-like hydroxyapatite (HA) is a classically-utilized and well tested modification for scaffold in bone tissue engineering as it mimics the biphasic structure of natural bone [17], and has shown to positively impact BMP2 signaling via improved release kinetics and new bone formation in rats and mice [18, 19]. Another route for improving BMP2 signaling is activating the endogenous BMP signaling pathway by using small molecules such as phenamil to act as a synergizing agent, which can help lower required dosage while remaining cost-effective [20–22]. Although the promising roles of HA and phenamil for improvement of BMPs-induced bone formation were reported in other scaffolds and systems [23–26], their effects and application to our newly developed TISA 3D PCL scaffolds remain unknown.

In this work, we study the capabilities of NF 3D PCL scaffolds modified with mineral-mimicking HA in combination with BMP2 activator phenamil and their effects on osteogenesis *in vitro* and bone formation *in vivo*. We hypothesize that by combining bone-matrix-biomimetic PCL/HA composite scaffolds and introducing a synergizing agent for BMP2 in phenamil, we can generate a bone-forming favorable niche, thereby significantly

Author Manuscript Author Manuscript Author Manuscript Author Manuscript

improving the efficacy of BMP2 to achieve adequate bone formation at relatively low dose of BMPs.

2. Experimental

2.1. Materials

Polycaprolactone (PCL, M w = 80,000), gelatin (G1890), ethanol, dichloromethane (DCM), N,N-dimethylformamide (DMF), were purchased from the Sigma-Aldrich (St. Louis, MO). All of the chemicals/materials were used without further purification.

2.2. Electrospinning and Scaffold Fabrication

As described in our previous work [15, 16], PCL NF mats with diameter ranging from 200 nm – 1 μm were generated *via* electrospinning process. The electrospinning setup included a high voltage power supply (Gamma High Voltage Research, Inc., Ormond Beach, FL) and a laboratory-produced roller (with the diameter of 25 cm). After mat synthesis, scaffolds were cut into individual nanofibers and tiny pieces upon mechanical grinding into liquid nitrogen repeatedly, until almost all of the short individual NF pieces were collected. Shortened nanofibers were placed into a glass bottle in a combined water/gelatin/ethanol solution (4/2/1 mL volume ratio) and submerged into a water bath at 55 °C for 3 min. During this time period, the short nanofibers and/or tiny pieces of PCL spontaneously agglomerated into a 3D structure. Immediately thereafter, the bottle/vial with PCL 3D agglomerate was placed into ice water for 30 min to prevent the further shrinkage and/or agglomeration. Finally, the obtained PCL 3D agglomerate was rinsed with DI water several times to remove the residual ethanol and gelatin.

2.3. HA Deposition via Simulated Body Fluid (SBF)

A 10x concentrated SBF solution was generated by adding several ions to 450 mL of DI water, after modification of formula described previously [27]. The ensuing solution was then adjusted to 500 mL using DI water, and pH adjusted to 6.0. For HA coating, scaffolds were immersed in the 10x SBF for 24 hours at 37°C. Scaffolds were then removed from the fluid and rinsed in DI water three times to remove any excess and unattached ions and then lyophilized overnight.

2.4. Mechanical Test

The elastic modulus of the electrospun material was determined using the atomic force microscope (AFM, Model: MFP-3D BIO, Asylum Research, Santa Barbara, CA) mounted on an inverted microscope (Model: IX73, Olympus America Inc). A silicon nitride tip (0.6 N/m) attached with a 5 μm diameter borosilicate sphere was used to indent the electrospun fibrous material at an indentation speed of 1 μm/s. Three different locations were measured for each sample. Young's modulus of the fibrous material was evaluated by fitting a modified Hertz model onto the AFM indentation curve using the built in function of AFM software (Asylum Research) [28].

Author Manuscript Author Manuscript Author Manuscript Author Manuscript

2.5. Surface and Morphological Characterization

A Zeiss Supra 40VP field-emission scanning electron microscope (SEM) was employed to characterize morphological structures of various samples [15, 16]. Scaffolds were sputter coated for 60 seconds prior to SEM for imaging purposes. Water surface contact angle was determined by use of VCA Optima goniometer and imaged using VCAOptimaXE software (AST Products Inc.). Scaffolds were fixed horizontally and a 2.0 μl drop of water was allowed to rest on the surface for 10 seconds before capturing images. The surface chemical compositions of scaffolds before and after SBF immersion were determined by attenuated total reflectance (ATR) spectroscopy (Nicolet, USA). The spectra were collected in transmission mode in the mid-IR range (4000–400 cm -1).

2.6. In vitro Cell Study

2.6.1. Sterilization and Cell Seeding—PCL NF scaffolds were first cut into discs (5 mm diameter × 2 mm thickness) with tissue punch, the samples were then immersed in 70% ethanol for 30 min followed by being washed with PBS for 3 times. Subsequently, these samples were incubated in minimum essential medium α (α-MEM, Gibco, Waltham, MA) for 30 min. The residual medium on a scaffold was removed with sterile gauzes before C2C12 cells were seeded into the scaffold (1×10ˆ5 cells per scaffold). All of the cells/scaffolds were cultured in 24-well plate at 37 °C with 5% CO2.

2.6.2. Cell Morphology and Viability—The mouse multipotent C2C12 cell was a generous gift from Dr. Yifan Li at the University of South Dakota. C2C12 morphologies on different scaffolds were visualized by Texas red-X Phalloidin (Molecular Probes, Grand Island, NY) and DAPI (SouthernBiotech, Birmingham, AL) staining methods, which respectively labels F-actin and cell nuclear [15, 16]. Cell viability on 3D scaffolds was assessed using the LIVE/DEAD cell imaging kit (Invitrogen #R37601) by following manufacturer's instructions. In brief, after culture in growth medium for 24 h, the constructs of cells/scaffolds were placed in sterile 4-well chambered coverglass (Lab-TekTM II, Thermo Scientific) and rinsed with DPBS. The mixed Green/Red dye was then added to stain cells, then samples were incubated for 15 min at 37 °C with 5% CO_2. After staining, the cells were supplied with fresh growth medium. Stained cells were imaged with a laser scanning microscope (FV1200, Olympus, Japan). The ratio of live cells (green) and dead cells (red) was measured using ImageJ software (NIH, Bethesda, MD).

2.6.3. ALP Activity—ALP activity was carried out using an EnzoLyte pNPP Alkaline Phosphatase Assay Kit (AnaSpec, San Jose, CA), as we previously described [15, 16] with some minor modifications. Briefly, cells/scaffolds were rinsed with PBS solution and lysed with lysis buffer for 12 min at room temperature. The lysate was then transferred into a tube and centrifuged for 15 min at 2500 g at 4 °C. The collected supernatant or standard solution (50 μL) was mixed with p-nitrophenyl phosphate and incubated for 30 min at 37 °C. Following the incubation, the reaction was stopped by adding 100 μL terminated liquid. ALP activity was measured at 405 nm and normalized against total protein content. The total protein content was measured with a BCA kit (Thermo Scientific™, Waltham, MA) according to the manufacture's instruction. ALP histochemistry was carried out using an Alkaline Phosphatase Staining Kit (Sigma) by manufacturer's instructions. Wells were fixed

Author Manuscript Author Manuscript Author Manuscript Author Manuscript

by Citrate-Acetone-Formalehyde mixture for 30 seconds, and then again rinsed with DI water for 45 seconds. Cells were then stained via a diazonium salt/Naphthol AS-Bl Alkaline solution for 15 minutes at room temperature, then once again rinsed for 2 minutes in DI water.

2.6.4. Gene Expression Analysis—Total RNA from scaffolds was isolated using a GeneJET™ RNA Purification Kit (Thermo Scientific™, Waltham, MA) by following manufacturer's instruction. RNA concentration was determined by absorbance at 260nm, where an equivalent amount per of RNA (0.5μg/group) was processed to generate cDNA using the High Capacity cDNA Reverse Transcript kit (Applied Biosystems, Forster City, CA). Quantitative PCR was performed with Taqman gene expression assays (Applied Biosystems, Forster City, CA) as our previously described [15, 16]. TaqMan® Gene Expression Assays of GAPDH (Mm99999915), Runx2 (mCG122221), and BSP (Mm00436767) were purchased from Applied Biosystems (Forster City, CA).

2.7. Bone Regeneration in vivo

2.7.1. In vivo Bone Formation—For *in vivo* bone regeneration, animal surgeries were performed according to the guidelines approved by the Institutional Animal Care and Use Committee (IACUC) of the University of South Dakota. Inbred C57BJL/6 male mice (5–6 weeks, Envigo) were adopted for the study. Mice were shaved and an antiseptic (70% ethanol) was applied to the surgical area. As per our previous protocol, each mouse received a total of 4 scaffolds on their dorsal sides [15]. Scaffolds received 2.5 μg BMP2 and/or 0.4 μg phenamil, which was re-suspended in 10μg of collagen I solution (Bedford, MA, USA). Mice were euthanized 28 days after surgery, and retrieved ossicles were fixed in 10% neutral buffered formalin for 2 days and then transferred to 70% ethanol until further analysis.

2.7.2. Radiographic & Histological Analysis—Radiographic analysis was performed on the fixed constructs using an In-Vivo Xtreme small animal imaging system (Bruker, Billerica, MA, USA). The formalin fixed ossicles were decalcified using 15% EDTA (pH = 7.2) solution for 1 day and then embedded in paraffin. Ten micron cross-sections were cut from the middle of scaffolds and stained with Hematoxylin and Eosin (H&E) for microscopic observation. The percentage of new bone area of each specimen was measured using the ImageJ software.

2.8. Statistical analysis and image editing

To determine statistical significance of observed differences between the study groups, a two-tailed homoscedastic t-test was applied. A value of $p < 0.05$ was considered to be statistically significant, while $0.05 < p < 0.10$ was considered to represent a nonsignificant, but clear trend in cell or tissue response. Values are reported as the mean ± one standard deviation (SD). Brightness and contrast were adjusted equally across all of the images for improved visibility.

Author Manuscript Author Manuscript Author Manuscript Author Manuscript

3. Results

3.1. Morphology of PCL/HA-3D scaffolds

As described in our previous work, 3D electrospun PCL scaffolds were generated through the innovative TISA method following by freeze drying, leaving 3D structure with interconnected and hierarchically structured porous structure [15]. Control PCL scaffolds possessed porosity of ~96% and pore sizes up to 300 μm, with fiber diameter in the ranges of 200 nm-1μm (Fig. 1, A–C). Observation by SEM revealed a uniform coating of HA crystals on PCL-3D scaffolds, both on the outside surface (Fig. 1, D–F) and inner cross section (G–I), with minimal obstruction of porous morphology noted.

3.2. Scaffold Surface Properties

2D electrospun mats are used for surface characterization due to difficulty using 3D TISA for contact angle goniometry and FTIR-ATR devices. As shown in Fig. 2, surface modification to PCL nanofiber mats (Fig. 2A) demonstrated a consistent HA-coating on the surface after 24h (Fig. 2B), indicating ease of precipitation for the 10x SBF solution. Wettability of scaffolds was measured to determine change in hydrophobicity, as a significant decrease in contact angle of ~30° from 130°to 99° was noted from PCL only (Fig. 2C) to PCL/HA (Fig. 2D). The crystalline material was examined by FTIR-ATR, revealing characteristic phosphate peaks at 1040 and 600–560 typical of hydroxyapatite as confirmed in prior literature [29].

3.3. Mechanical properties of PCL/HA-3D scaffolds

The Young's modulus was measured after PCL scaffolds were modified with HA, yielding an increase from 6438±342 N to 13032±404 N (Fig. 2F). Mechanical testing was initially observed using a 1kN electromechanical tester, yielding no significant difference in sample modulus (data not shown); further investigation was undergone with AFM to discover more local modulus of individual fibers/smaller areas. Upon investigation with AFM, PCL/HA-3D scaffolds were found to have significantly increased Young's modulus ($P < 0.05$).

3.4. ALP activity of cells exposed to phenamil

To study the effect of phenamil on osteogenic differentiation of C2C12 cells in culture, cells were cultured in medium containing varying concentrations of phenamil to observe response in ALP activity and potential toxicity. Resulting ALP quantification (Fig. 3A) showed phenamil alone induced a dose-dependent effect, with the most effective concentration at 20μM in solution, as significant cytotoxicity at 50 μM was noted (Fig. 3B). Subsequently, BMP2 was introduced and its effect in combination with phenamil was observed; histochemical analysis (Fig. 4A) showed phenamil was able to induce more intense ALP staining of C2C12 cells after 5d of culture in both high (100 ng/mL) and low (50 ng/mL) doses of BMP2. The combination effect was consistently noted in the quantification assay (Fig. 4B), as the two molecules induced a significantly higher ALP level (BMP2+Phe) in cells than either one separately.

Author Manuscript Author Manuscript Author Manuscript Author Manuscript

3.5. Cell morphology and viability on PCL-3D and PCL/HA-3D scaffolds

Morphologies of C2C12 cells on PCL-3D and PCL/HA-3D scaffolds were investigated after 24h of culture (Fig. 5). More bright cytoskeletal staining was observed in HA-modified groups (Fig. 5, B, E) compared to the control scaffolds (PCL-3D, Fig. 5, A, D). Both groups had roughly similar nuclear density and cell penetration into scaffolds, as evident in the 3D constructed z-stacked images (Fig. 5, D, E). Additionally, viabilities of C2C12 cells on PCL-3D and PCL/HA-3D scaffolds were quantitatively measured after culture for 24 by live/dead assay. As Fig. 5C shows, no significant difference was found in cell viability, indicating that addition of HA to PCL-3D scaffolds did not impact viability for cell life and growth.

3.6. Osteogenic differentiation of C2C12 cells on PCL-3D and PCL/HA-3D scaffolds

To study the effect of the HA-modification as well as phenamil on osteogenic differentiation of C2C12 cells, cells were cultured on either scaffold (with our without HA modification) in either growth medium or medium containing 20μM phenamil for 10 days. As an early osteogenic marker, ALP activity was quantitatively measured in scaffolds (Fig. 6A). Compared to control samples, addition of phenamil or HA induced a significant increase ($P < 0.05$) in ALP activity, indicating that both components are able to induce osteogenesis to some degree. The combined effect of both HA and phenamil further increased the activity to an even more significant degree, also suggesting the effects of these 2 components can be compounded. Showing consistent trends with the ALP data, quantitative gene expression results also indicated that both HA and phenamil could positively increase osteogenic differentiation of C2C12 cells on the scaffolds; early gene marker Runx2 showed a similar trend (Fig. 6B), and mature osteogenic marker Bone Sialoprotein (BSP) (Fig. 6C) also demonstrated significant increases in phenamil and HA groups and a further increase in combined component effect on gene expression.

3.7. Ectopic bone formation on PCL/HA-3D scaffolds

To study the effects of our scaffolds influence in BMP2-induced bone formation *in vivo*, PCL-3D and PCL/HA-3D scaffolds were implanted ectopically on the dorsal sides of mice for up to 4 weeks. Scaffolds of PCL or PCL/HA were supplemented with BMP2, phenamil, or a combination of the two to observe the singular and combination effect of the experimental variables. Radiographic examination of scaffolds after harvesting revealed a trending increase of opacity of samples from positive control with BMP2 only (Fig. 7A), as addition of HA (Fig. 7B) revealed a slight increase in opacity, and a further and significant increase was noted with combination of phenamil and HA added to scaffolds (Fig. 7D). Scaffolds without BMP2 (Fig. 7C) possessed little to no bone formation, suggesting that BMP2 is a required component for ectopic bone formation *in vivo.* Histological observation indicated a similar trend to radiopacity, as some new bone was formed in positive control group with BMP2 (Fig. 8A), and experimental groups adding HA (Fig. 8B) and HA/phenamil (Fig. 8D) yielded significantly more new bone as evident in the microscope images. New bone area was quantified by ImageJ software (Fig. 8E), detailing the average increase of new bone which was significantly more ($P < 0.05$) in each group starting with control of BMP2 only, increasing with addition of HA and further with HA+phemamil. Also

Author Manuscript Author Manuscript Author Manuscript Author Manuscript

agreeing with radiopacity data was the lack of new bone formed in HA+phenamil only scaffolds without BMP2, as no bone was found in any samples from this group and neither HA nor phenamil could induce bone formation on PCL-3D scaffolds (data not shown).

4. Discussion

One of the critical challenges in bone regeneration is the necessity for high doses of BMP2 in tissue engineering strategies, leading to unintended side effects and high costs for treatments [30]. As we know drug/growth factor delivery is one of the three components of tissue engineering alongside scaffold materials and stem cells, it is likely we can use some improvements in other components to help lessen the workload and requirement of exogenous BMP2 delivery to see improved osteogenesis and new bone formation. Our previous work has shown the ability to generate 3D NF electrospun scaffolds via an innovative and convenient approach of TISA, which had also shown capability for blend with PLA for further improved bioactivity, however discussion noted that significant improvements to bioactivity and growth factor signaling could yield stronger BMP2-induced osteogenesis and new bone formation, as the new bone formation of the scaffolds was significant yet limited in area[15, 16]. In this work, bone-like HA was adopted for its similarity to native bone environment, and the small molecule phenamil was used for its ability to improve and synergize with the BMP2 signaling pathway. Due to the nature of bio-inertness and hydrophobicity of PCL, a 10x concentrated simulated body fluid was used to precipitate HA crystals throughout the PCL-3D scaffolds, after a simple test on the as-electrospun mats to confirm deposition was performed. Small molecule phenamil was utilized as a BMP2 activator for its cost effectiveness and ease of use, as its ability to promote BMP2 signaling pathway has been outlined in previous research [21]. The resulting combination of PCL/HA-3D scaffolds with initial administration of phenamil showed a significant increase in new bone formation in *in vivo* mouse models, and each modification showed improved osteogenic effects *in vitro* as well.

Biomimicking of nature and its organisms is a long practiced strategy, with its origins dating all the way back to da Vinci’s time during the Renaissance [31]. As bone is a primarily biphasic material consisting of an organic (collagen) and inorganic phase (hydroxyapatite), a logical improvement on our 3D-PCL NF scaffolds would be to incorporate bone-like mineral into the matrix to imitate a more natural bone-like niche. This incorporation has been utilized in previous bone tissue engineered research, and would improve bioactivity and wettability of our scaffolds, as well as provide a more biomimicking ECM akin to natural bone, assisting stem cell growth and differentiation [10, 23, 32]. As seen in our *in vitro* data, significant improvements in osteogenic factors such as ALP activity, and osteogenic gene markers Runx2/BSP were noted in PCL/HA-3D scaffolds versus control PCL-3D scaffolds. This could be attributed simply to addition of bioactive HA, as scaffolds morphology and especially porous morphology remained uncompromised during modification with HA. Additionally, mechanical strength was noticeably increased as shown by AFM data, another factor has been shown to contribute to increased osteogenic differentiation of stem cells and bone formation as we reported previously [33]. It was noticed that the local stiffness may be more directly influencing the cell behaviors compared to the bulk mechanical strength of the scaffolds, which were not significantly changed by HA modification as shown by our data.

Author Manuscript Author Manuscript Author Manuscript Author Manuscript

Water contact angle was also noticeably decreased, with lowered hydrophobicity of scaffolds possibly playing into increased osteogenic differentiation of cells on PCL/HA-3d scaffolds. Consistently, more intense cytoskeletal staining was observed on the HA-modified scaffolds, suggesting stronger cell attachment on PCL/HA-3D scaffolds possibly contribute to the improved osteogenic differentiation as well [34, 35].

In addition to bulk/surface modification by HA, it was noted in our cell culture studies that the small molecule phenamil could induce osteogenic differentiation in C2C12 cultures, as varied amounts of phenamil showed a dose-dependent response of ALP activity on cells alone. In addition, phenamil was able to improve ALP activity of low doses of BMP2 when used in tandem, as the combination effect showed noticeable increase over both phenamil and BMP2 alone. Even in the absence of BMP2, *in vitro* studies showed similar ALP increase with combination treatment of phenamil on PCL/HA-NF scaffolds, suggesting both of these factors are able to positively increase osteogenic differentiation to some degree. It is known that phenamil increases BMP2 signaling by downregulating Smurf1 and increasing SMAD signaling, and prior research has utilized this small molecule to induce osteoblastic differentiation of stem cells and mineralization of MSCs, and shown its feasibility in combination use with BMP2 for further improved osteogenic applications[20–22]. As a widely used cell line, C2C12 is a pre-myoblast with the ability to differentiate to osteoblast with the presence of BMPs. Due to the high sensitivity to BMPs, C2C12 is a valuable tool to evaluate the osteo-inductive activity of drugs or materials [36, 37]. Therefore, our study provided further evidence to indicate that phenamil is a promising small molecule with osteo-inductivity that can both induce osteogenic differentiation and improve BMP2-induced osteoblast differentiation in a common and relative homogenous cell line, C2C12, compared to primary cells.

Our *in vivo* results followed a similar trend to our *in vitro* data; PCL/HA-3D scaffolds in combination with phenamil were able to see markedly increased osteogenic capabilities, generating significantly more bone in our ectopic mouse model. It was remarkable that the relatively small amount of phenamil in a bolus dose was able to achieve such a significant increase (1:6 ratio, phenamil: BMP2 by weight), suggesting this molecule can be an extremely cost effective way to increase new bone formation in combination with BMP2 and HA modification. Consistent with prior research [21, 22, 38] and our previous work however, we found that phenamil alone is not enough to generate new bone structures in scaffolds, despite seeing increased osteogenic effects from *in vitro* data alone, in addition to HA modification as well. However, these factors used in combination with the essential and FDA approved BMP2 molecule yielded significant increase to new bone formation on scaffolds, suggesting these factors are able to cooperatively and synergistically enhance BMP2 signaling. Furthermore, as this experiment utilized bolus dosage strategies, drug delivery mechanisms to deliver consistent therapeutic over longer period of time could yield even further favorable results; whereby this is a possible avenue for future experiments. Additionally, *in vivo* cranial defect models may be adopted in future studies, as they provide a more clinically relevant defect scenario for studies.

Author Manuscript Author Manuscript Author Manuscript Author Manuscript

5. Conclusions

A novel 3D electrospun PCL/HA NF composite scaffold was generated to mimic natural bone matrix, and utilized in combination with the BMP2 activator molecule phenamil for improved osteogenesis *in vitro* and new bone formation *in vivo.* Both our *in vitro* and *in vivo* results indicated that PCL/HA-3D scaffolds and phenamil molecule were able to form a synergistic core to generate more favorable microenvironments for osteogenic differentiation and BMP2-induced ectopic bone formation than previously reported 3D electrospun PCL NF scaffolds. Overall, our results suggest that PCL/HA-3D scaffolds in combination with phenamil provide highly favorable microenvironments for BMP2-induced bone formation.

Acknowledgments

This work was supported by the EPSCoR program of National Science Foundation (Award No.: IIA-1335423) and by the Competitive Research Grant program of South Dakota Board of Regents (Award No.: UP1500172, UP1600205). The authors would like to acknowledge the assistance provided by the Sanford Research Imaging Core and Molecular Pathology Core, which were supported by the COBRE grants of National Institutes of Health (Grant No.: P20 GM103620 and P20 GM103548). The authors would also thank Dr. Erin B. Harmon for his outstanding technical assistance.

References

1. Schroeder JE, Mosheiff R. Tissue engineering approaches for bone repair: concepts and evidence. Injury. 2011; 42:609–613. [PubMed: 21489529]
2. Khosla S, Westendorf JJ, Oursler MJ. Building bone to reverse osteoporosis and repair fractures. J Clin Invest. 2008; 118:421–428. [PubMed: 18246192]
3. Zheng Z, Yin W, Zara JN, Li W, Kwak J, Mamidi R, Lee M, Siu RK, Ngo R, Wang J, Carpenter D, Zhang X, Wu B, Ting K, Soo C. The use of BMP-2 coupled -Nanosilver-PLGA composite grafts to induce bone repair in grossly infected segmental defects. Biomaterials. 2010; 31:9293–9300. [PubMed: 20864167]
4. Haidar ZS, Hamdy RC, Tabrizian M. Delivery of recombinant bone morphogenetic proteins for bone regeneration and repair. Part B: Delivery systems for BMPs in orthopaedic and craniofacial tissue engineering. Biotechnol Lett. 2009; 31:1825–1835. [PubMed: 19690811]
5. Sheikh Z, Javaid M, Hamdan N, Hashmi R. Bone Regeneration Using Bone Morphogenetic Proteins and Various Biomaterial Carriers. Materials. 2015; 8:1778. [PubMed: 28788032]
6. Martino MM, Briquez PS, Maruyama K, Hubbell JA. Extracellular matrix-inspired growth factor delivery systems for bone regeneration. Adv Drug Deliv Rev. 2015; 94:41–52. [PubMed: 25895621]
7. Ma PX. Biomimetic Materials for Tissue Engineering. Adv Drug Deliv Rev. 2008; 60:184–198. [PubMed: 18045729]
8. Dong X, Wang Q, Wu T, Pan H. Understanding Adsorption-Desorption Dynamics of BMP-2 on Hydroxyapatite (001) Surface. Biophys J. 2007; 93:750–759. [PubMed: 17617550]
9. Kuboki Y, Jin Q, Takita H. Geometry of carriers controlling phenotypic expression in BMP-induced osteogenesis and chondrogenesis. J Bone Joint Surg Am. 2001; 83-A(Suppl 1):S105–115.
10. Liu X, Smith LA, Hu J, Ma PX. Biomimetic nanofibrous gelatin/apatite composite scaffolds for bone tissue engineering. Biomaterials. 2009; 30:2252–2258. [PubMed: 19152974]
11. Kaushik SN, Kim B, Walma AM, Choi SC, Wu H, Mao JJ, Jun HW, Cheon K. Biomimetic microenvironments for regenerative endodontics. Biomater Res. 2016; 20:14. [PubMed: 27257508]
12. Jiang YC, Jiang L, Huang A, Wang XF, Li Q, Turng LS. Electrospun polycaprolactone/gelatin composites with enhanced cell-matrix interactions as blood vessel endothelial layer scaffolds. Mater Sci Eng C Mater Biol Appl. 2017; 71:901–908. [PubMed: 27987787]
13. Wang X, Ding B, Li B. Biomimetic electrospun nanofibrous structures for tissue engineering. Mater Today (Kidlington). 2013; 16:229–241. [PubMed: 25125992]

Author Manuscript Author Manuscript Author Manuscript Author Manuscript

14. Wang J, Valmikinathan CM, Liu W, Laurencin CT, Yu X. Spiral-structured, nanofibrous, 3D scaffolds for bone tissue engineering. J Biomed Mater Res A. 2010; 93:753–762. [PubMed: 19642211]
15. Xu T, Miszuk JM, Zhao Y, Sun H, Fong H. Electrospun polycaprolactone 3D nanofibrous scaffold with interconnected and hierarchically structured pores for bone tissue engineering. Adv Healthc Mater. 2015; 4:2238–2246. [PubMed: 26332611]
16. Yao Q, Cosme JG, Xu T, Miszuk JM, Picciani PH, Fong H, Sun H. Three dimensional electrospun PCL/PLA blend nanofibrous scaffolds with significantly improved stem cells osteogenic differentiation and cranial bone formation. Biomaterials. 2017; 115:115–127. [PubMed: 27886552]
17. Venkatesan J, Kim SK. Nano-hydroxyapatite composite biomaterials for bone tissue engineering–a review. J Biomed Nanotechnol. 2014; 10:3124–3140. [PubMed: 25992432]
18. Wang J, Chen Y, Zhu X, Yuan T, Tan Y, Fan Y, Zhang X. Effect of phase composition on protein adsorption and osteoinduction of porous calcium phosphate ceramics in mice. J Biomed Mater Res A. 2014; 102:4234–4243. [PubMed: 24497384]
19. He X, Liu Y, Yuan X, Lu L. Enhanced healing of rat calvarial defects with MSCs loaded on BMP-2 releasing chitosan/alginate/hydroxyapatite scaffolds. PLoS One. 2014; 9:e104061. [PubMed: 25084008]
20. Park KW, Waki H, Kim WK, Davies BS, Young SG, Parhami F, Tontonoz P. The small molecule phenamil induces osteoblast differentiation and mineralization. Mol Cell Biol. 2009; 29:3905–3914. [PubMed: 19433444]
21. Fan J, Im CS, Cui ZK, Guo M, Bezouglaia O, Fartash A, Lee JY, Nguyen J, Wu BM, Aghaloo T, Lee M. Delivery of Phenamil Enhances BMP-2-Induced Osteogenic Differentiation of Adipose-Derived Stem Cells and Bone Formation in Calvarial Defects. Tissue Eng Part A. 2015; 21:2053–2065. [PubMed: 25869476]
22. Lo KW, Ulery BD, Kan HM, Ashe KM, Laurencin CT. Evaluating the feasibility of utilizing the small molecule phenamil as a novel biofactor for bone regenerative engineering. J Tissue Eng Regen Med. 2014; 8:728–736. [PubMed: 22815259]
23. Brun V, Guillaume C, Mechiche Alami S, Josse J, Jing J, Draux F, Bouthors S, Laurent-Maquin D, Gangloff SC, Kerdjoudj H, Velard F. Chitosan/hydroxyapatite hybrid scaffold for bone tissue engineering. Biomed Mater Eng. 2014; 24:63–73. [PubMed: 24928919]
24. Morelli S, Salerno S, Holopainen J, Ritala M, De Bartolo L. Osteogenic and osteoclastogenic differentiation of co-cultured cells in polylactic acid-nanohydroxyapatite fiber scaffolds. J Biotechnol. 2015; 204:53–62. [PubMed: 25858154]
25. Bhattacharjee P, Naskar D, Maiti TK, Bhattacharya D, Kundu SC. Investigating the potential of combined growth factors delivery, from non-mulberry silk fibroin grafted poly(ε-caprolactone)/hydroxyapatite nanofibrous scaffold, in bone tissue engineering. App Mater Today. 2016; 5:52–67.
26. Ruan Z, Yao D, Xu Q, Liu L, Tian Z, Zhu Y. Effects of mesoporous bioglass on physicochemical and biological properties of calcium sulfate bone cements. App Mater Today. 2017
27. Kokubo T, Takadama H. How useful is SBF in predicting in vivo bone bioactivity? Biomaterials. 2006; 27:2907–2915. [PubMed: 16448693]
28. Darling EM. Force scanning: a rapid, high-resolution approach for spatial mechanical property mapping. Nanotechnology. 2011; 22:175707. [PubMed: 21411911]
29. Stanić V, Janaćković D, Dimitrijević S, Tanasković SB, Mitrić M, Pavlović MS, Krstić A, Jovanović D, Raičević S. Synthesis of antimicrobial monophase silver-doped hydroxyapatite nanopowders for bone tissue engineering. App Surface Sci. 2011; 257:4510–4518.
30. Charles LF, Woodman JL, Ueno D, Gronowicz G, Hurley MM, Kuhn LT. Effects of low dose FGF-2 and BMP-2 on healing of calvarial defects in old mice. Exp Gerontol. 2015; 64:62–69. [PubMed: 25681640]
31. Taylor R. Reflecting the impossible. Nature. 2009; 460:462–462.
32. Milovac D, Gallego Ferrer G, Ivankovic M, Ivankovic H. PCL-coated hydroxyapatite scaffold derived from cuttlefish bone: morphology, mechanical properties and bioactivity. Mater Sci Eng C Mater Biol Appl. 2014; 34:437–445. [PubMed: 24268280]

Author Manuscript Author Manuscript Author Manuscript Author Manuscript

33. Sun H, Zhu F, Hu Q, Krebsbach PH. Controlling stem cell-mediated bone regeneration through tailored mechanical properties of collagen scaffolds. Biomaterials. 2014; 35:1176–1184. [PubMed: 24211076]

34. Qian Y, Chen H, Xu Y, Yang J, Zhou X, Zhang F, Gu N. The preosteoblast response of electrospinning PLGA/PCL nanofibers: effects of biomimetic architecture and collagen I. Int J of Nanomed. 2016; 11:4157–4171.

35. Yun YP, Lee JY, Jeong WJ, Park K, Kim HJ, Song JJ, Kim SE, Song HR. Improving Osteogenesis Activity on BMP-2-Immobilized PCL Fibers Modified by the γ-Ray Irradiation Technique. BioMed Research Int. 2015; 2015:302820.

36. Katagiri T, Yamaguchi A, Komaki M, Abe E, Takahashi N, Ikeda T, Rosen V, Wozney JM, Fujisawa-Sehara A, Suda T. Bone morphogenetic protein-2 converts the differentiation pathway of C2C12 myoblasts into the osteoblast lineage. J Cell Biol. 1994; 127:1755–1766. [PubMed: 7798324]

37. Yao Q, Sandhurst ES, Liu Y, Sun H. BBP-functionalized biomimetic nanofibrous scaffolds can capture BMP2 and promote osteogenic differentiation. J of Mat Chem B. 2017; 5:5196–5205.

38. Fan J, Guo M, Im CS, Pi-Anfruns J, Cui ZK, Kim S, Wu BM, Aghaloo TL, Lee M. Enhanced Mandibular Bone Repair by Combined Treatment of Bone Morphogenetic Protein 2 and Small-Molecule Phenamil. Tissue Eng Part A. 2017; 23:195–207. [PubMed: 27771997]

Author Manuscript Author Manuscript Author Manuscript Author Manuscript

Highlights

- 3D electrospun PCL/hydroxyapatite nanofibrous composite scaffolds were developed.
- These scaffolds had high porosity and interconnected hierarchically structured pores.
- Both in vitro osteogenic differentiation and in vivo bone formation were improved by phenamil and bone-like scaffold.
- The scaffolds could act as favorable synthetic ECM for bone regeneration

Author Manuscript Author Manuscript Author Manuscript Author Manuscript

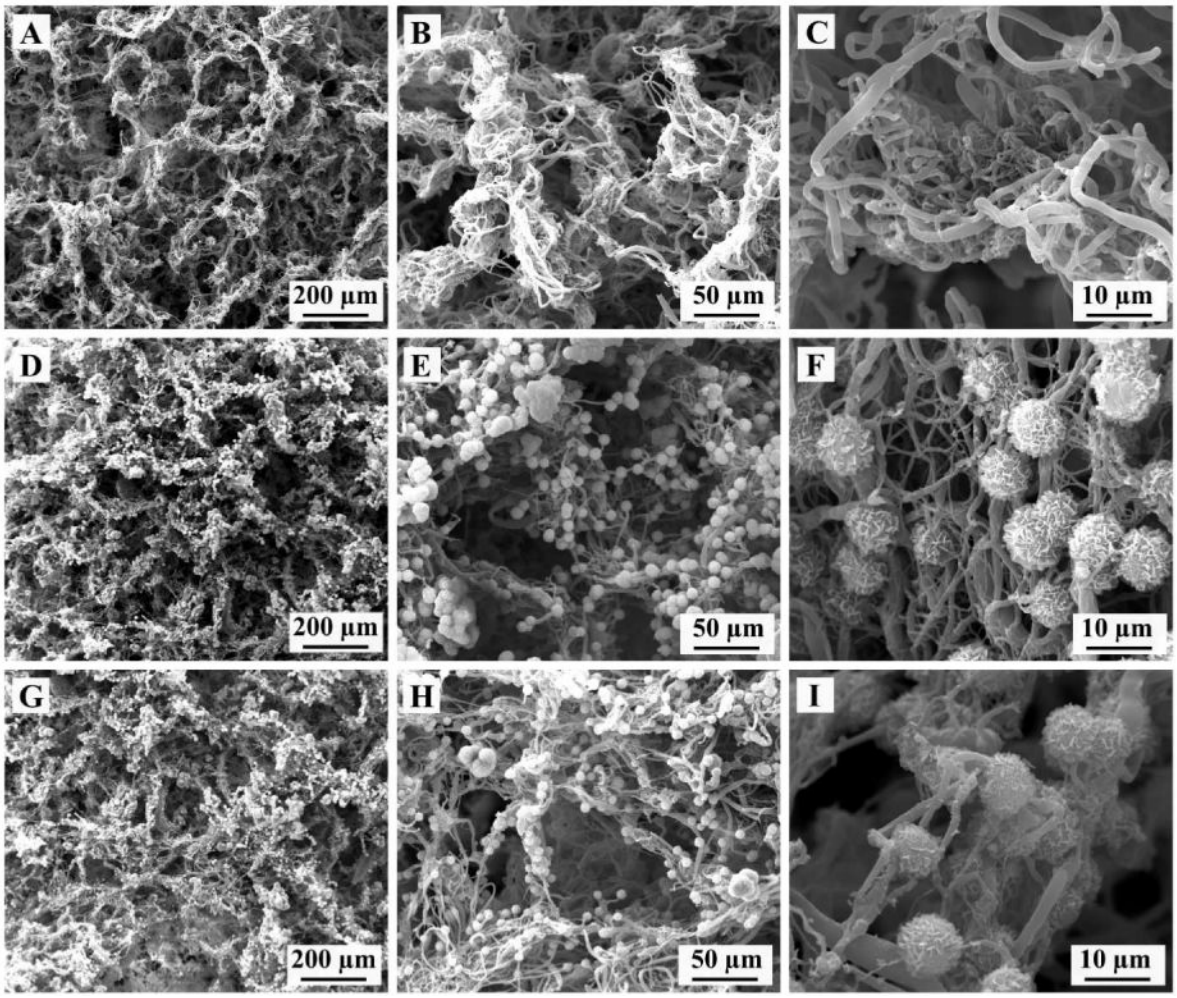

Fig. 1.

SEM images showing representative morphologies of PCL-3D scaffolds (A–C) and PCL/HA coated scaffolds external surface (D–F) and internal cross section (G–I).

Author Manuscript Author Manuscript Author Manuscript Author Manuscript

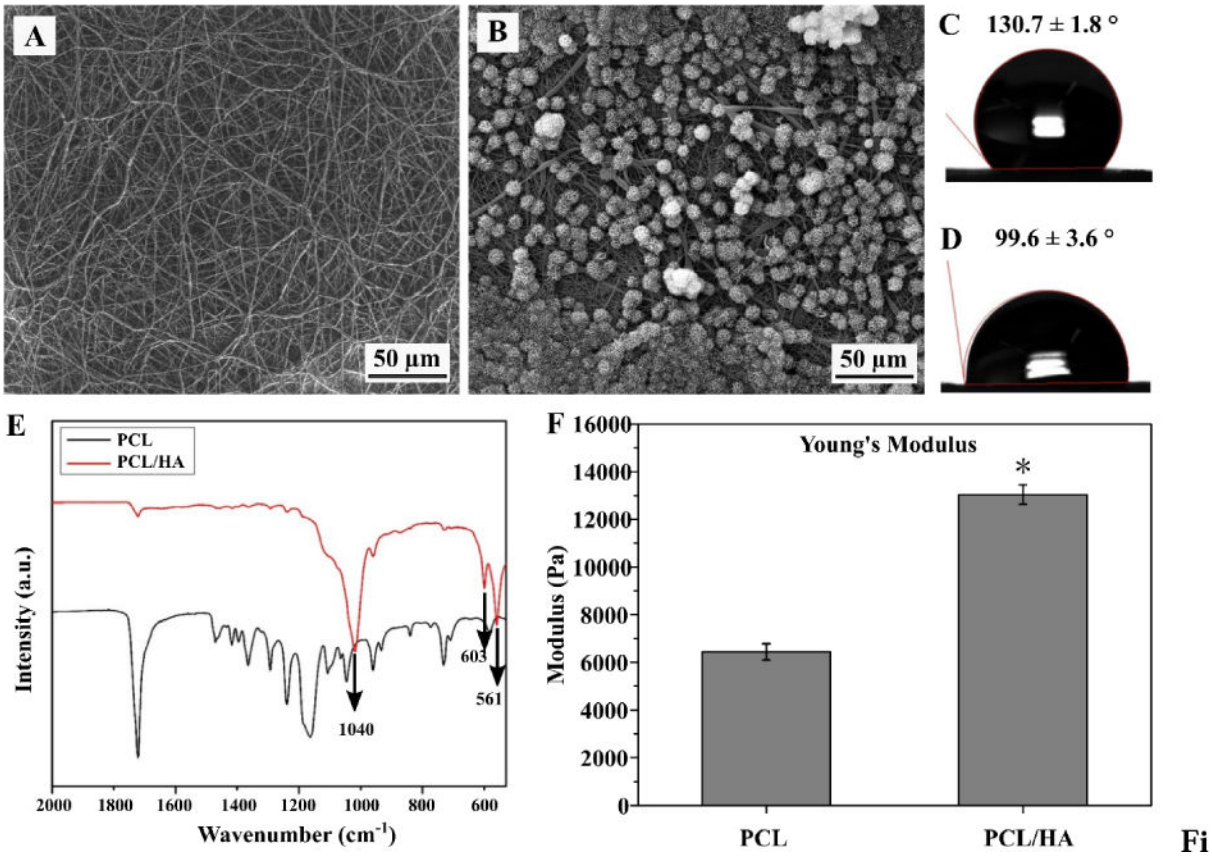

Fig. 2.

SEM of NF PCL mats both before (A) and after (B) soaking in SBF for 24h. Contact angle of corresponding neat (C) and HA-coated (D) scaffolds as measured by contact angle goniometer. ATR spectra of scaffolds prior to and after SBF treatment (E). Young's Modulus of PCL-3D and PCL/HA-3D scaffolds as measured by AFM (F). Data are expressed as mean ± SD (n = 3).

Author Manuscript Author Manuscript Author Manuscript Author Manuscript

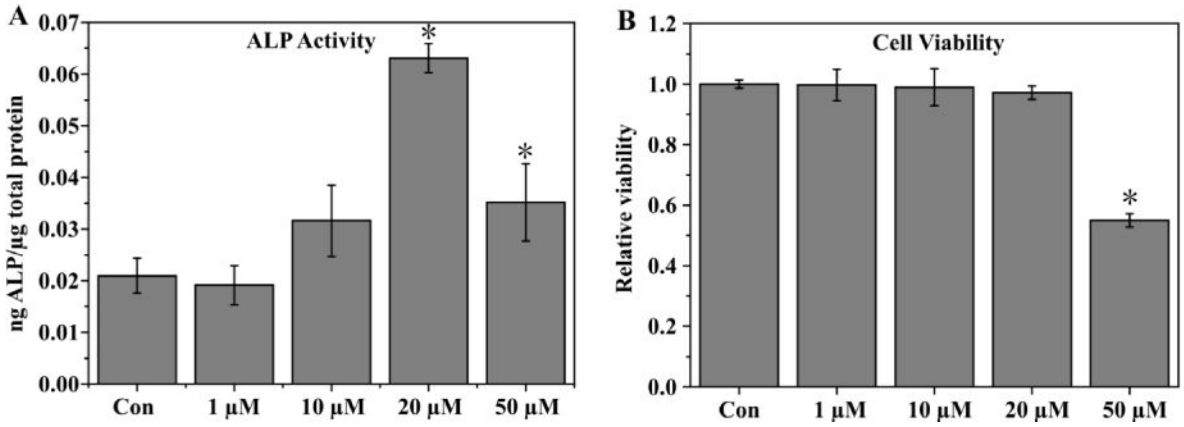

Fig. 3.

ALP activity of C2C12 cells cultured in medium containing varying levels of phenamil as measured after 5d (A), viability of cells as measured by MTS assay (B). Activity is normalized by total protein content. Data are expressed as mean ± SD (n =3).

Author Manuscript Author Manuscript Author Manuscript Author Manuscript

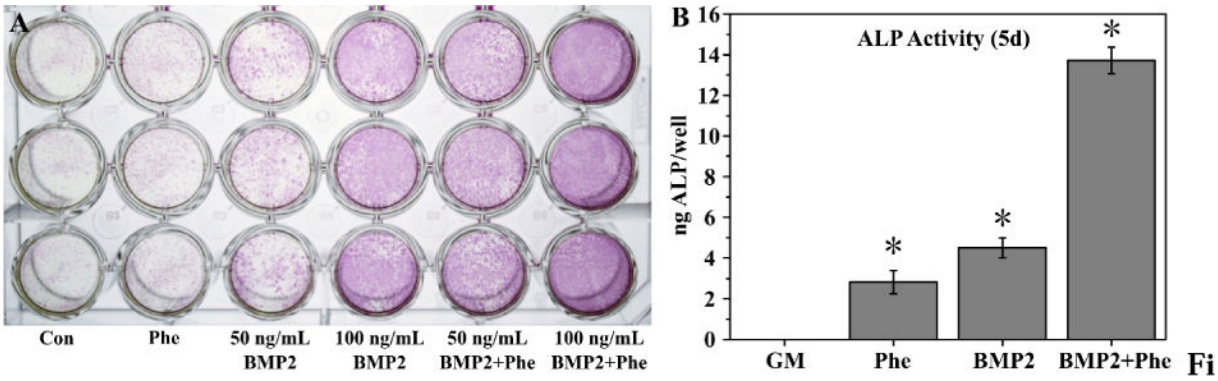

Fig. 4.

ALP staining (A) of cells after culture in growth medium containing phenamil (20 μM) and/or BMP2 (50 ng/mL or 100 ng/mL). Quantitative measurement of ALP in wells containing phenamil or BMP2 or combination of both (B). Data are expressed as mean ± SD (n =3).

Author Manuscript Author Manuscript Author Manuscript Author Manuscript

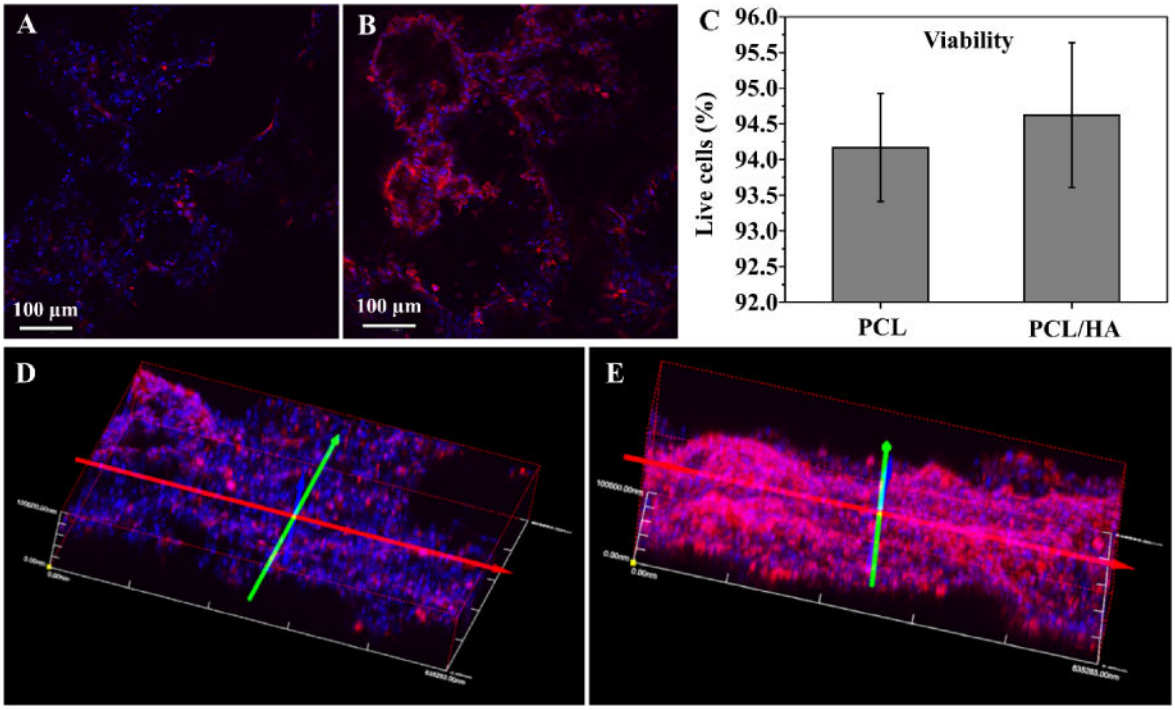

Fig. 5.

C2C12 cell morphologies on PCL-3D (A) and PCL/HA-3D scaffolds (B) after 24h of culture. Cell viabilities on both scaffolds after 24h of culture (C) and 3D stacked image of 100 μm sections of PCL-3D (D) and PCL/HA-3D (E) are also shown. Data are expressed as mean ± SD (n = 3). Scale bars (A and B) = 100 μm.

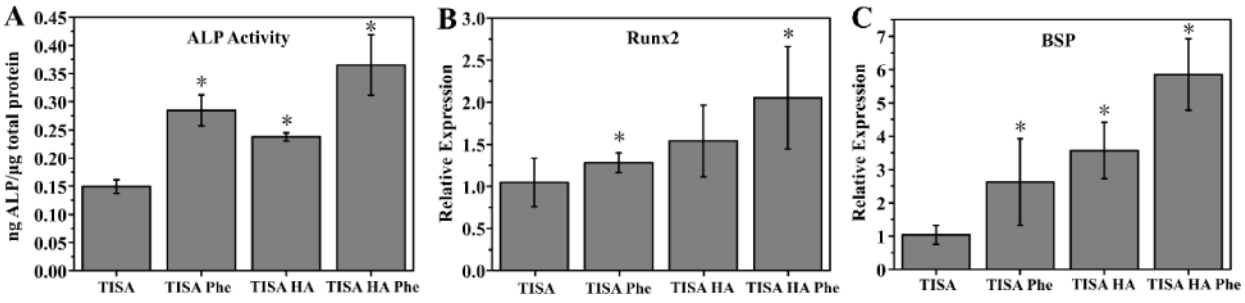

Fig. 6.

ALP activity of C2C12 cells cultured in PCL and PCL/HA 3D scaffolds after 7 days in growth medium with or without phenamil (A). Osteogenic gene markers Runx2 (B) and BSP (C) were measured by real-time PCR assays after culturing for 10 days. Data are expressed as mean ± SD ($n = 3$).

Author Manuscript Author Manuscript Author Manuscript Author Manuscript

Author Manuscript Author Manuscript Author Manuscript Author Manuscript

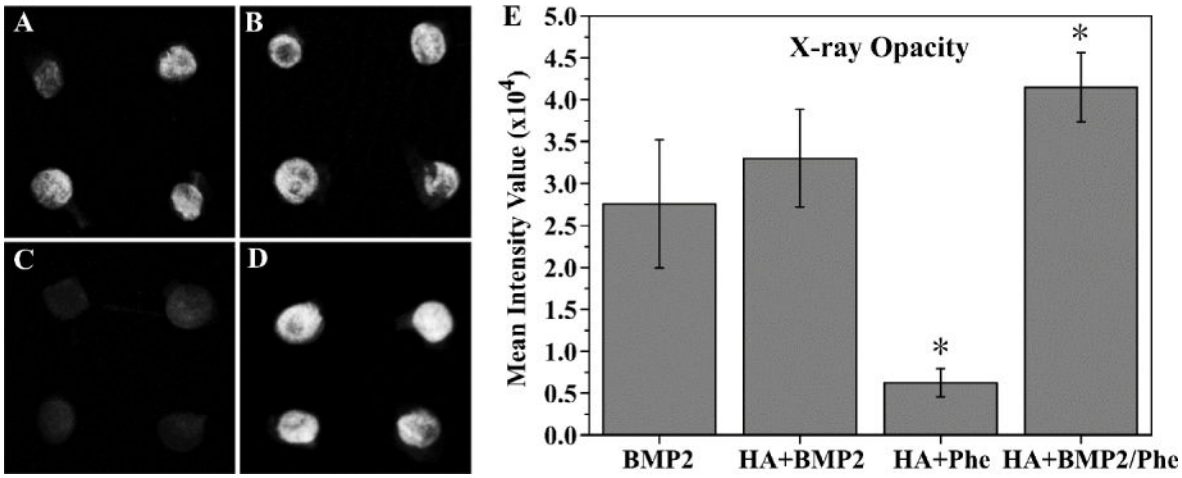

Fig. 7.

Radiographic examination of ossicles (A–D) after harvesting from mice after 4 weeks. BMP2 only group (A), BMP2 + HA group (B), phenamil + HA group (C), and BMP2/phenamil + HA group (D) were all imaged, and mean intensity value of scaffolds was quantified (E). Data are expressed as mean ± SD ($n = 4$).

Author Manuscript Author Manuscript Author Manuscript Author Manuscript

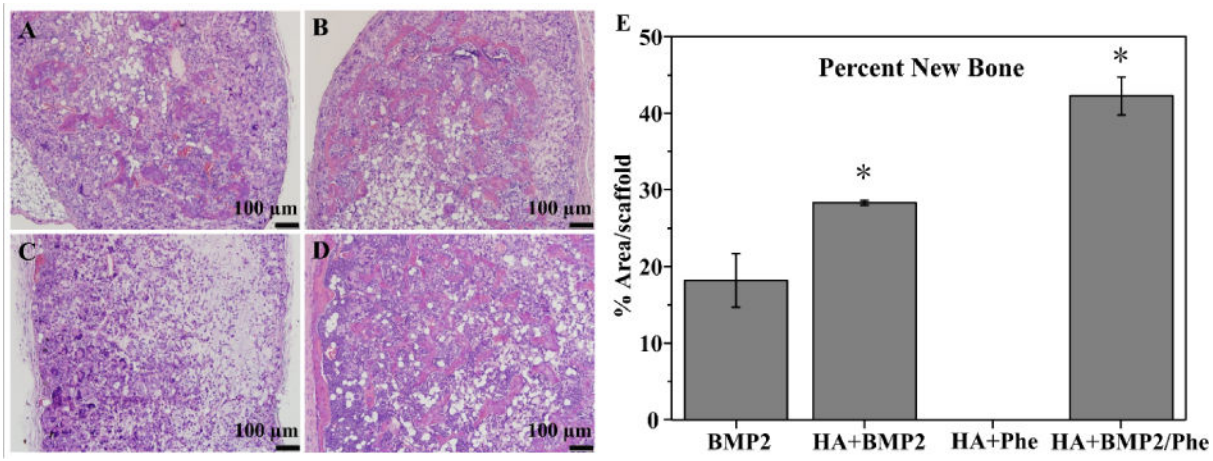

Fig. 8.

H&E staining of retrieved ossicles after 4 weeks implantation *in vivo.* BMP2 only group (A), BMP2 + HA group (B), phenamil + HA group (C), and BMP2/phenamil + HA group (D) area of new bone was measured by ImageJ software (E). Scale bars = 100 μm.